JLB

Article

Endogenous and exogenous pathways maintain the reductive capacity of the phagosome

Dale R. Balce, Catherine J. Greene,* Pankaj Tailor,* and Robin M. Yates*,†,1*

*Department of Comparative Biology and Experimental Medicine, Faculty of Veterinary Medicine, and †Department of Biochemistry and Molecular Biology, Faculty of Medicine, University of Calgary, Alberta, Canada

RECEIVED MARCH 2, 2015; REVISED OCTOBER 30, 2015; ACCEPTED DECEMBER 4, 2015. DOI: 10.1189/jlb.2HI0315-083R

ABSTRACT

Although endosomes, lysosomes, and phagosomes require a reductive environment for the optimal activity of disulfide reductases and other thiol-dependent enzymes, how these reductive environments are established and maintained remain unknown. Our goal in this study was to begin to elucidate the redox control systems responsible for maintaining redox-sensitive enzymatic activities in the phagolysosome of murine macrophages. Through the use of specific inhibitors and genetic knockdown of known redox enzymes, we identified redox pathways that influence phagosomal disulfide reduction. In particular, known inhibitors of the NADPH-dependent selenoprotein, thioredoxin reductase, were shown to inhibit phagosomal disulfide reduction and phagosomal proteolysis. This was supported by the observation that conditional deletion of the selenocysteine tRNA in macrophages decreased phagosomal disulfide reduction capacity. In addition, pharmacologic inhibition of the pentose phosphate pathway decreased rates of disulfide reduction and proteolysis in the phagosome, implicating NADPH as a source of phagosomal reductive energy. Finally, by analyzing the effect of extracellular redox couples, such as cysteine:cystine on thiol-dependent phagosomal processes, we demonstrated that the extracellular space can additionally supply the phagosome with reductive energy. Collectively, these data demonstrate that defined cytosolic reductive pathways act in concert with the uptake of cysteine from the extracellular space to support thiol-dependent chemistries in the phagosome. *J. Leukoc. Biol.* 100: 17–26; 2016.

Introduction

Phagosomal disulfide reductases act in concert with phagosomal proteases to efficiently degrade internalized material and process protein-based antigens [1]. Phagosomal protein degradation is tightly regulated at multiple levels, including the delivery of enzymes to the phagosome, zymogen processing, and enzyme pH optima [2]. Recently, the redox control of lysosomal Cys cathepsins has been added as an additional level of regulation of phagosomal proteolysis [3, 4]. The active-site thiol of the Cys cathepsins (Cys25; papain numbering) must be in a reduced state for proteolytic activity, but it is susceptible to oxidation—particularly during phagosomal generation of ROS [5]. Phagosomal disulfide reduction is largely catalyzed by the thiol-dependent enzyme, known as GILT [6, 7]. Similarly to the Cys cathepsins, GILT relies on reduced active-site Cys residues to carry out the reduction of disulfide bonds (Cys46/Cys49 in murine GILT) [8]. Hence, efficient proteolysis and disulfide reduction (2 key processes in antigen processing) are reliant on a reductive microenvironment within the phagolysosome and the availability of reducing equivalents. Despite the accepted and well-cited importance of the reductive properties of endosomes, lysosomes, and phagosomes for antigen processing and basic cellular function [1, 6, 9, 10], how these vesicles establish and maintain their redox homeostasis was hitherto completely unknown.

In contrast to the unknowns of endo/lysosomal redox maintenance, cytosolic redox pathways have been well characterized. Generally, redox homeostasis of the cytosol (in addition to a number of organelles) is largely determined by the TR/Trx and the GR/GSH systems that operate within all eukaryotic cells [11]. In both systems, NADPH, generated through the pentose phosphate pathway, delivers electrons/reducing equivalents to the flavoproteins TR or GR, which then transfer reductive energy to Trx and GSH, respectively. Thus, reductive energy flow follows the generation of a source of reductive energy and the transfer of reductive energy from the source to effector enzymes/molecules

Abbreviations: $^{-/-}$ = deficient/knockout, 6-AN = 6-aminonicotinamide, ATG = aurothioglucose, ATM = aurothiomalate, BMMØ = bone marrow-derived macrophage, BSO = buthionine sulfoximine, Cybb = B6.129S6-Cybb, Cys = cysteine, CySS = cystine, DNCB = 1-chloro-2,4-dinitrobenzene, DPI = diphenyleneiodonium, DQ-albumin = DQ Green BODIPY albumin, fl/fl = floxed, GILT = γ-IFN-inducible lysosomal thiol

(*continued on next page*)

The online version of this paper, found at www.jleukbio.org, includes supplemental information.

1. Correspondence: Dept. of Comparative Biology and Experimental Medicine, Faculty of Veterinary Medicine, University of Calgary, 3330 Hospital Dr., NW, HRIC 4AA10, Calgary, AB, Canada T2N 4N1. E-mail: rmyates@ucalgary.ca

by intermediate redox factors. Whether these pathways contribute reductive energy to endosomes, lysosomes, and phagosomes to maintain redox balance in the lumen of these vesicles or if these vesicles are dependent on other redox control systems is currently unknown and constitutes a gap in the fundamental understanding of these organelles [12, 13].

The objective of this study was to begin to elucidate potential redox control systems that contribute to the reductive capacity of the phagosome by targeting known cellular/extracellular sources of reducing equivalents and specific cytosolic redox pathways. Through a hypothesis-neutral, bioactive molecule-based screen and the use of selective inhibitors, we identified TR or TR-related enzyme as potential intermediate redox factors and NADPH as a potential source of reducing equivalents involved in maintaining phagosomal reductive capacity. Furthermore, we demonstrated that deletion of *Trsp* diminished phagosomal disulfide reduction in macrophages, implicating selenoproteins in the maintenance of phagosomal thiol-dependent processes. Finally, we demonstrated that extracellular Cys, but not GSH, at physiologic concentrations additionally acts to bolster phagosomal disulfide reduction. Collectively, this evidence demonstrates that defined endogenous and exogenous redox pathways provide reductive energy to the phagosome and support thiol-dependent chemistries within the phagosomal lumen.

MATERIALS AND METHODS

Animals and cells

C57BL/6 (WT) mice and the congenic mouse strains Cybb$^{-/-}$ and B6.129P2-Lyz2$^{tm1(cre)Ifo}$/J (*LysM-Cre* transgenic C57BL/6) were purchased from The Jackson Laboratory (Bar Harbor, ME, USA). The C57BL/6 mouse line carrying the *Trsp*$^{fl/fl}$ gene was kindly provided by Dr. Dolph Hatfield (National Institutes of Health, Bethesda, MD, USA) [14]. Mouse lines were strategically bred to obtain *Trsp*$^{fl/fl}$*/LysM-Cre*$^{+/-}$ and *Trsp*$^{fl/fl}$*/LysM-Cre*$^{-/-}$ littermate controls. The following primers were used to assess deletion of the *Trsp* in tails and fully differentiated BMMØs: CKNO2, 5′-GCAACGGCAGGTGTCGC-TCTGCG-3′, and CKNO8RP, 5′-CGTGCTCTCTCCACTGGCTCA-3′ (to detect WT *Trsp*, *Trsp*$^{fl/fl}$, and deleted *Trsp*) [14]. All animal experiments were conducted according to protocols approved by the University of Calgary Animal Use and Care Committee. C57BL/6 and Cybb$^{-/-}$ BMMØs were differentiated and cultured as described previously [15]. BMMØs, derived from Trsp$^{fl/fl}$/LysM-Cre$^{-/-}$ and Trsp$^{fl/fl}$/LysM-Cre$^{+/-}$ mice, were differentiated in the presence of BMMØ media, supplemented with 500 μM 2-ME (Sigma-Aldrich, St. Louis, MO, USA), and plated for analysis, 7 d after bone marrow isolation to minimize potential phenotypes associated with generalized perturbations to cellular redox physiology.

Assessment of phagosomal lumenal chemistries

IgG-opsonized 3.0 μm experimental particles bearing various fluorescent reporters were prepared and used for phagosomal lumenal assessment in BMMØs, as described previously [15]. All assays were performed in an assay buffer consisting of PBS supplemented with 1 mM $CaCl_2$, 2.7 mM KCl, 0.5 mM $MgCl_2$, 5 mM dextrose, and 0.25% gelatin. In brief, phagosomal rates of disulfide reduction were evaluated by measuring the dequenching of particle-bound BODIPY FL L-CySS (Life Technologies, Carlsbad, CA, USA) relative to the Alexa Fluor 594 SE calibration fluor using a FLUOstar OPTIMA microplate reader (BMG Labtech, Ortenberg, Germany) or EnVision multilabel reader (PerkinElmer Life Sciences, Waltham, MA, USA). DQ-albumin, covalently bound to experimental particles, were used to monitor phagosomal proteolysis using a FLUOstar OPTIMA microplate reader or a FlexStation microplate reader (Molecular Devices, Sunnyvale, CA, USA). Phagosomal pH was calculated by recording the ratio of the fluorescence emissions at 520 nm particle-bound carboxyfluorescein SE (Life Technologies), excited at 490 and 450 nm, respectively, using a FLUOstar OPTIMA microplate reader, followed by polynomial regression to a standard curve, as described previously [15]. Phagosome-specific ROS production was performed by monitoring the degree of particle-bound OxyBURST H_2HFF- oxidation using an EnVision multilabel reader [16]. RFUs, defined by the equation, RFU = SF^{RT}/CF (where SF^{RT} indicates substrate fluorescence in real time, and CF indicates calibration fluorescence), were plotted against time. To calculate relative rates, the slopes (as described by the equation, $y = mx + c$, where y = RFU, m = slope, $c = y$ intercept, and x = time) of the linear portion of the relative substrate fluorescence plotted against time were calculated relative to the internal control indicated. To measure the release of H_2O_2 into the supernatant, BMMØ monolayers were washed and then incubated for 1 h in assay buffer containing 10 mg/ml serum-opsonized zymosan (Sigma-Aldrich). Amplex UltraRed (Life Technologies), at a final concentration of 10 ng/ml plus 1 unit horseradish peroxidase (Sigma-Aldrich), was added to each well supernatant postzymosan exposure and incubated for 15 min. Amplex UltraRed fluorescence was monitored using a GENios Pro microplate reader (Tecan Group, Maennedorf, Switzerland).

Use of ICCB compound library and individual inhibitors

Treatment of BMMØs, with the ICCB Known Bioactives library (BIOMOL), was performed as described previously [17]. In brief, fully differentiated BMMØs were plated onto μ-clear 96-well assay plates (Greiner Bio-One, Kremsmünster, Austria), 18 h before phagosomal assessment. Cells were washed and incubated with compounds or DMSO (vehicle) controls, 1 h before the assessment of phagosomal disulfide reduction. The screen was performed in duplicate as separate experiments. Relative rates of disulfide reduction were compared with untreated vehicle (DMSO) controls. Compounds that overtly affected macrophage health, inhibited phagocytosis of experimental particles (as assessed microscopically post-treatment), or severely altered general phagosomal parameters of maturation (such as pH and/or phago/lysosomal fusion, as performed previously [17]) were excluded from further analysis. Treatment of BMMØs with ATG (Sigma-Aldrich) and ATM (Sigma-Aldrich) at the given concentrations was performed for 1 h before phagosomal assessment. Treatment of BMMØs with DNCB (Sigma-Aldrich) at the given concentrations was performed for 30 min before phagosomal assessment. BMMØs were treated with 6-AN (Cayman Chemical, Ann Arbor, MI, USA) or BSO (Sigma-Aldrich) at the given concentrations for a duration of 24 h before phagosomal assessment. With the exception of 6-AN and BSO, all compounds were kept in the assay medium for the duration of phagosomal assessment.

NADPH/total thiol quantification in BMMØs

WT and Cybb$^{-/-}$ BMMØs were plated in 24-well plates and seeded with/without 1 mM 6-AN, 24 h before lysate preparation. Cell lysate preparation and measurement of NADPH were performed using the NADP/NADPH Quantification Kit (Sigma-Aldrich), as per the manufacturer's instructions. Absorbance at 450 nm was recorded by use of an EnVision multilabel reader (PerkinElmer Life Sciences). Total cellular thiol concentrations, following BSO treatment, were performed by lysing the cells in 1% SDS containing 100 μM 5,5′-DTNB [18, 19]. Absorbance indicating thiol labeling was measured at 412 nm with an EnVision multilabel reader.

(*continued from previous page*)

reductase, GR = glutathione reductase, GSH = glutathione, GSSG = glutathione disulfide, ICCB = Harvard Institute of Chemistry and Cell Biology, LysM = lysozyme M, NOX2 = NADPH oxidase 2, RFU = relative fluorescent unit, ROS = reactive oxygen species, SE = succinimidyl ester, TR = thioredoxin reductase, Trsp = selenocysteine tRNA gene, Trx = thioredoxin, WT = wild-type

Reconstituted TR activity assays

Inhibition of TR by ATG, ATM, DPI, curcumin, and DNCB was assessed using a TR colorimetric kit, based on TR-mediated reduction of 5,5′-DTNB (Cayman Chemical). Activity of purified rat liver TR in the presence of compounds at the indicated concentrations was measured according to the manufacturer's instructions.

Phagosomal measurements in the presence of varying extracellular thiol:disulfide concentration/ratios

BMMØs were exposed to assay buffer supplemented with increasing concentrations of thiol:disulfide ratios immediately before and for the duration of phagosomal assessment. To emulate extracellular oxidizing thiol: disulfide conditions, BMMØs were exposed to increasing concentrations of Cys:CySS at a molar ratio of 1:5 (1 μM Cys:5 μM CySS, 10 μM Cys:50 μM CySS, and 100 μM Cys:500 μM CySS, corresponding to ~0.1×, ~1×, and ~10× of the physiologic concentration, respectively); GSH:GSSG at a ratio of 20:1 (0.28 μM GSH:0.014 μM GSSG, 2.8 μM GSH:0.14 μM GSSG, and 28 μM GSH:1.4 μM GSSG); or a combination of both redox couples. To emulate an intracellular, relatively reducing Cys:CySS ratio, BMMØs were exposed to increasing concentrations of Cys:CySS at a molar ratio of 4:1 (1 μM Cys:0.25 μM CysSS, 10 μM Cys:2.5 μM CysSS, 100 μM Cys:25 μM CySS). Cys, CySS, GSH, and GSSG were purchased from Sigma-Aldrich.

Online Supplemental material

Supplemental Table 1 presents raw data obtained from the ICCB library disulfide reduction screen. Supplemental Fig. 1 presents representative real-time traces of select compounds from the screen shown to influence phagosomal disulfide reduction and TR inhibition by compounds in a reconstituted system. Supplemental Fig. 2 shows the effect of the TR inhibitor DNCB on phagosomal disulfide reduction, proteolysis, and acidification. Supplemental Fig. 3 shows the effect of GSH depletion on both phagosomal disulfide reduction and proteolysis.

RESULTS

A bioactive chemical-based screen of phagosomal disulfide reduction identified compounds that are known to target cytosolic redox pathways

As very little is known about the pathways that contribute to the reductive capacity of the phagosomal lumen, we conducted a hypothesis-neutral screen using bioactive compounds to focus the subsequent study of potential redox pathways in an unbiased fashion. The screen was performed by monitoring the rates of phagosomal disulfide reduction of a particle-bound fluorogenic substrate BODIPY FL L-CySS in BMMØs in the presence of 480 arrayed compounds represented in the ICCB Known Bioactives library. Reduction of the self-quenched BODIPY FL L-CySS-based substrate was monitored by an increase in fluorescence emission (as a result of dequenching of the BODIPY substrate upon reduction of the disulfide) following phagocytosis of IgG-opsonized, substrate-conjugated experimental particles [20]. BODIPY FL L-CySS has been shown to efficiently measure phagosome-specific disulfide reduction, and GILT$^{-/-}$ BMMØs display a marked reduction in the ability to process this substrate [7]. As the production of phagosomal ROS negatively influences phagosomal disulfide reduction [17], we performed the disulfide reduction screen with BMMØs derived from Cybb$^{-/-}$ mice that lack the gp91^{phox} subunit of the NOX2 complex. Compounds that modulated rates of phagosomal disulfide reduction without overtly affecting other nonredox-dependent phagosomal features (particularly acidification and phagosome-lysosome fusion [17]) were chosen for subsequent analysis. The primary screen identified several compounds that modulated rates of phagosomal disulfide reduction (Supplemental Table 1). Most notably, these included compounds that were known or reported to affect TR. For instance, rates of phagosomal disulfide reduction were decreased by curcumin (a reported TR inhibitor [21]) and DPI (a flavoprotein inhibitor [22]) and were enhanced by ebselen (an organo-selenium compound that is known to enhance the catalytic efficiency of TR [23–25]; Supplemental Fig. 1). Inhibition of purified TR activity by curcumin and DPI was confirmed in a reconstituted system (Supplemental Fig. 1D).

ATG and ATM inhibit phagosomal disulfide reduction

Preliminary findings from the screen indicated that TR or TR-like enzymes (such as GR) may impact phagosomal disulfide reduction and potentially other lysosomal thiol-dependent processes. Thus, we observed the effect of the gold-based, TR-selective inhibitors, ATG and ATM, on phagosomal disulfide reduction [26–28]. We chose ATG and ATM, historically used for the treatment of rheumatoid arthritis, as we found that they were well tolerated by cultured macrophages, as opposed to similar compounds, such as auranofin [26]. ATG and ATM dramatically decreased phagosomal disulfide reduction in BMMØs derived from NOX2$^{-/-}$ mice in a dose-dependent manner (**Fig. 1A–D**). To observe the effect of ATG/ATM on phagosomal proteolysis, we used IgG-opsonized experimental particles bearing the proteolytic, self-quenched substrate, DQ-albumin, which has been shown to efficiently measure the activity of Cys, aspartic, and serine proteases [29]. In particular, it has been validated as a suitable substrate for the phagosomal, thiol-dependent protease, cathepsin S, as BMMØs, deficient in cathepsin S, show a 50% reduction in the rate of DQ-albumin hydrolysis within the phagosome [7]. Both ATG and ATM, at concentrations that completely abolished disulfide reduction, also decreased phagosomal proteolysis, albeit to a lesser extent (Fig. 1E–G). As Cys cathepsins mediate a large proportion of phagosomal proteolysis and additionally require a reductive lumenal environment for optimal activity, the observed decrease in phagosomal proteolysis is consistent with the oxidation of the phagosomal microenvironment by ATG and ATM, although the direct inhibition of phagosomal proteases cannot be ruled out [30]. To ensure that the effects of ATG/ATM were not a result of any major defects in phagosomal maturation, we evaluated the ability of phagosomes to acidify in the presence of ATG/ATM. No significant differences were observed in the rates or extents of phagosomal acidification in ATG- or ATM-treated BMMØs (Fig. 1H–J). In addition, we evaluated the impact on phagosomal disulfide reduction by TR inhibition with the chemically unrelated, TR-selective alkylating agent DNCB [31, 32]. Phagosomal disulfide reduction was decreased significantly in NOX2$^{-/-}$ BMMØs treated with 5 μM DNCB (Supplemental Fig. 2). At this concentration, phagosomal acidification and phagosomal proteolysis were not altered significantly. Specific inhibition of purified TR activity by ATG/ATM and DNCB was confirmed in a reconstituted system (Supplemental Fig. 1D and **Fig. 2G**). Together, these results suggest that TR or enzymes related to TR

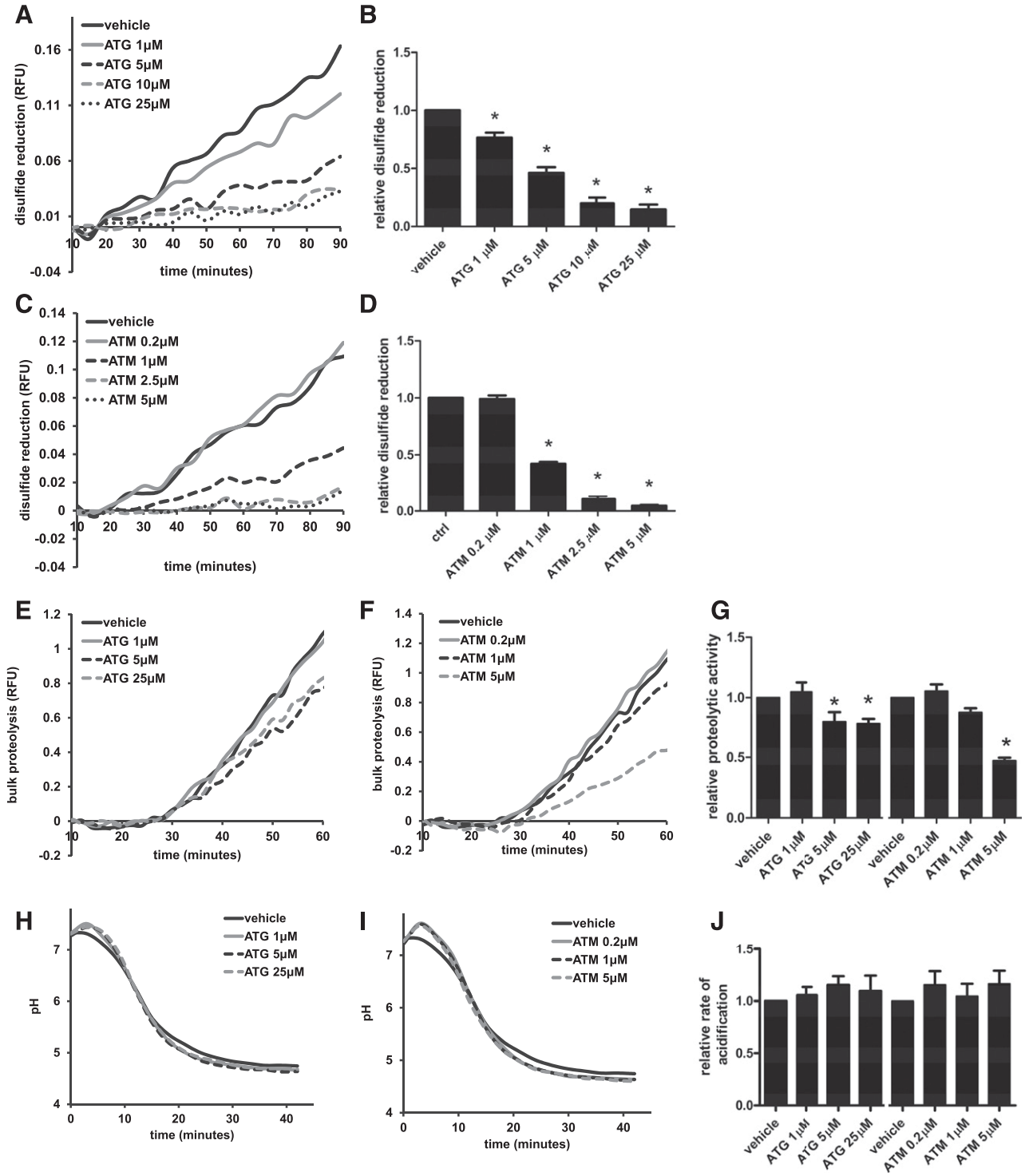

Figure 1. ATG and ATM dramatically decrease phagosomal disulfide reduction. BMMØs, derived from Cybb$^{-/-}$ mice, were incubated for 1 h in the presence of ATG/ATM at the indicated concentrations or DMSO control before assessment of phagosomal disulfide reduction. (A–D) Phagosomal disulfide reduction of the BODIPY FL L-CySS substrate conjugated to IgG-opsonized experimental particles. (E–G) Phagosomal proteolysis of the DQ-albumin substrate conjugated to IgG-opsonized experimental particles. (H–J) Phagosomal pH calculated from excitation ratios of the pH-sensitive carboxyfluorescein-SE conjugated to experimental particles by regression to a standard curve. (A, C, E, F, H, and I) Representative real-time traces. RFU values are proportional to the degree of substrate reduction/proteolysis. (B, D, G, and J) Averaged rates relative to untreated controls (ctrl) of 3 independent experiments are shown for each phagosomal measurement. Average relative rates of disulfide reduction and proteolysis were calculated between 40 and 60 min after particle internalization. Relative rates of phagosomal acidification were calculated between 10 and 15 min after particle internalization. Error bars denote SEM of 3 independent experiments. *$P < 0.05$.

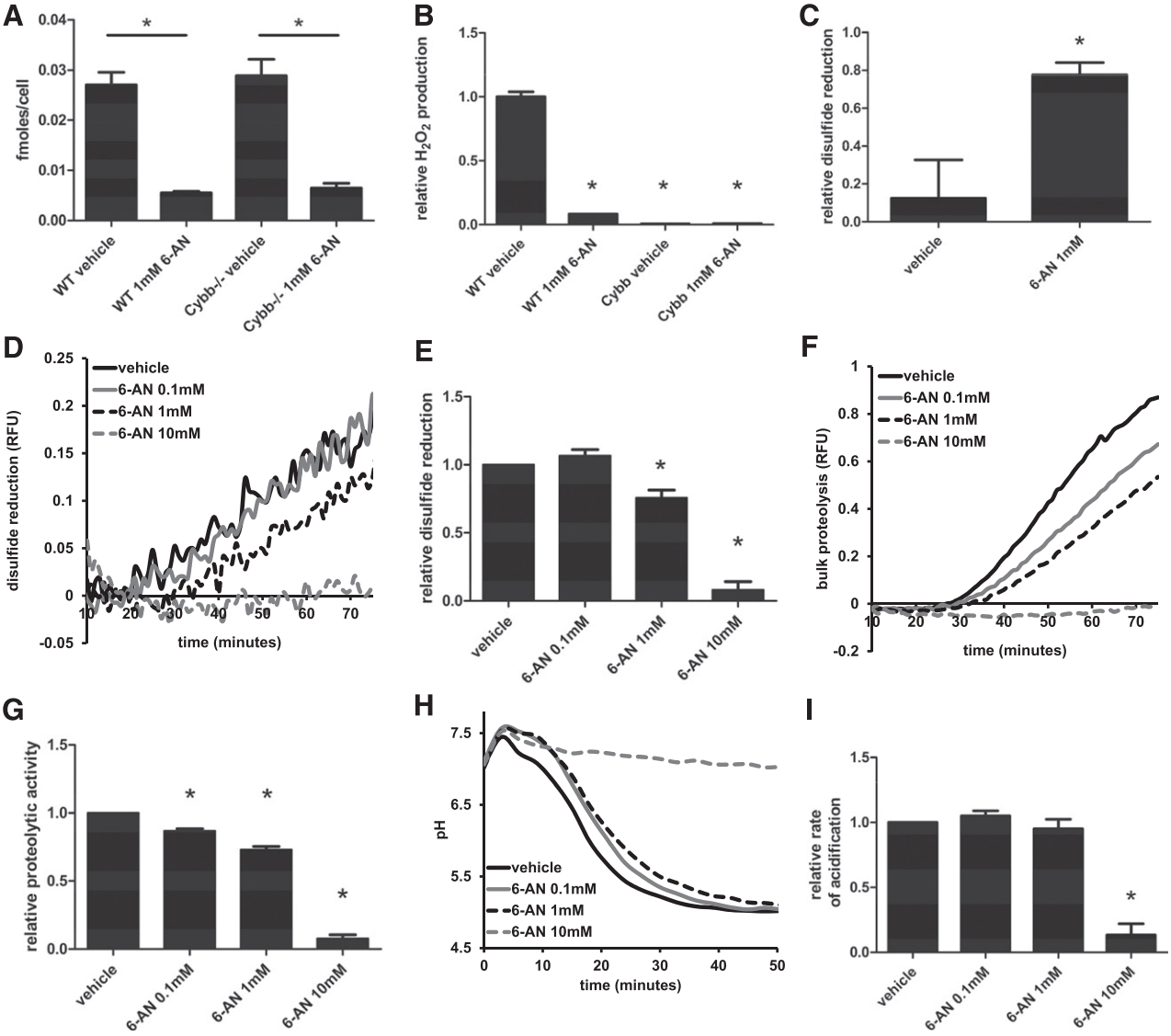

Figure 2. NADPH depletion affects phagosomal disulfide reduction and proteolysis. BMMØs, derived from Cybb$^{-/-}$ mice, were incubated for 24 h in the presence of the indicated concentrations of 6-AN or vehicle control before assessment of phagosomal disulfide reduction. (A) NADPH quantification in WT and Cybb$^{-/-}$ BMMØs treated with 1 mM 6-AN (4 independent experiments). (B) Extracellular H_2O_2 production in WT and Cybb$^{-/-}$ BMMØs treated with 1 mM 6-AN (4 independent experiments). (C) Phagosomal disulfide reduction of the BODIPY FL L-CySS substrate conjugated to IgG-opsonized experimental particles in WT BMMØs pretreated with 6-AN. (D and E) Phagosomal disulfide reduction of the BODIPY FL L-CySS substrate conjugated to IgG-opsonized experimental particles in Cybb$^{-/-}$ BMMØs pretreated with 6-AN. (F and G) Phagosomal proteolysis of the DQ-albumin substrate conjugated to IgG-opsonized experimental particles in Cybb$^{-/-}$ BMMØs pretreated with 6-AN. (H and I) Phagosomal pH calculated from excitation ratios of the pH-sensitive carboxyfluorescein-SE conjugated to experimental particles by regression to a standard curve. (D, F, and H) Representative real-time traces. RFU values are proportional to the degree of substrate reduction/proteolysis. (C, E, G, and I) Averaged rates relative to untreated controls of 3 independent experiments shown for each phagosomal measurement. Average relative rates of disulfide reduction and proteolysis were calculated between 40 and 60 min after particle internalization. Relative rates of phagosomal acidification were calculated between 10 and 15 min after particle internalization. Error bars denote SEM of 3–4 independent experiments. *$P < 0.05$.

may play a role in supporting disulfide reduction within phagosomes.

NADPH depletion affects phagosomal disulfide reduction and proteolysis

Phagosomal-reductive capacity must be maintained by a source of reducing equivalents. The cellular sources of reducing equivalents to the phagosome are yet to be defined. As NADPH is the source of reducing equivalents for TR, GR, and other cellular redox processes, we evaluated the effect of NADPH depletion on phagosomal disulfide reduction and proteolytic activity. 6-AN is known to deplete cellular levels of NADPH through inhibition of the pentose phosphate pathway [33]. Treatment of WT and Cybb$^{-/-}$ BMMØs with 1 mM 6-AN decreased relative amounts of NADPH by 86.0 ± 0.018% and 85.6 ± 0.015%, respectively (Fig. 2A). Unsurprisingly, treatment of WT BMMØs with 6-AN caused

a decrease in NOX2-dependent production of ROS (as NOX2 is dependent on NADPH; Fig. 2B). This resulted in a subsequent increase in phagosomal disulfide reduction (Fig. 2C), as disulfide reduction has been shown to be diminished dramatically during ROS production [17]. Thus, to observe NOX2-independent changes in phagosomal disulfide reduction as a result of NADPH depletion, BMMØs, derived from NOX2 deficient mice ($Cybb^{-/-}$), were used. Treatment of $Cybb^{-/-}$ BMMØs with 1 mM 6-AN resulted in a significant decrease in disulfide reduction and proteolysis (24.3 ± 5.6%; Fig. 2D and E) and 26.9 ± 2.2% (Fig. 2F and G, respectively). At this concentration, 6-AN had no effect on the ability of phagosomes to acidify, demonstrating that the decreases in disulfide reduction and proteolysis were not a result of any general defect in phagosome formation or maturation (Fig. 2H and I). To determine if NADPH is acting through the NADPH-dependent GR/GSH system, cells were treated with the inhibitor of GSH synthesis, BSO [34]. Treatment of $Cybb^{-/-}$ BMMØs with BSO, at concentrations that decreased total cellular thiol concentrations, had no effect on phagosomal disulfide reduction or proteolysis (Supplemental Fig. 3A–C). These results identify NADPH as a source of reducing equivalents that influence phagosomal, thiol-dependent processes in a GSH-independent fashion. This may occur through the activity of NADPH-dependent cellular reductases, such as TR.

Depletion of selenocysteine-containing enzymes decreases phagosomal disulfide reduction

Selenoenzymes play major roles in cellular antioxidant functions. This family of redox enzymes (that includes TR) relies on the modified amino acid, selenocysteine, as a redox-active residue [35]. To investigate the potential involvement of TR and other selenoenzymes in phagosomal thiol-dependent processes, we used a cre-lox system to conditionally knock out the *Trsp* in BMMØs. Heterozygous expression of the cre recombinase, under the LysM promoter, was sufficient to excise the $Trsp^{fl/fl}$ allele in fully differentiated BMMØs (**Fig. 3A**). As the redox balance in these cells is likely to be compromised as a result of the lack of major cellular antioxidants, we measured H_2O_2 levels produced on internalization of serum-opsonized zymosan particles. As expected, when selenoproteins were conditionally knocked down in BMMØs ($Trsp^{fl/fl}$/LysM-$Cre^{+/-}$), there was an overall increase in H_2O_2 released into the culture supernatant in response to the phagocytosis of zymosan (Fig. 3B). Interestingly, phagosome-specific measurements of OxyBURST H_2HFF substrate oxidation were not altered significantly, indicating that ROS production, at the level of the phagosome, remained unchanged in the absence of the selenoproteome (Fig. 3C). The increased release of H_2O_2 to the supernatant but unchanged levels of ROS in the phagosome in selenoprotein-deficient BMMØs is consistent with reduced cytosolic scavenging of H_2O_2 as a result of the depletion of selenocysteine-dependent GSH peroxidases (which constitute a large proportion of the selenoproteome of macrophages) [36]. Supportive of a role for selenoproteins, such as TR in the reductive maintenance of lysosomes, phagosomal disulfide reduction was decreased in $Trsp^{fl/fl}$/LysM-$Cre^{+/-}$ BMMØs (29.7 ± 3.0%; Fig. 3D and E) in the presence of the NOX2 inhibitor DPI compared with cre negative BMMØ controls ($Trsp^{fl/fl}$/LysM-$Cre^{-/-}$). Although we observed that DPI inhibits phagosomal disulfide reduction at 10 μM (Supplemental Fig. 1), 0.5 μM DPI was sufficient to inhibit NOX2-mediated ROS production without overtly affecting rates of phagosomal disulfide reduction, which permitted evaluation of disulfide reduction in the absence of ROS in the $Trsp^{fl/fl}$/LysM-$Cre^{-/-}$ BMMØs. No significant differences were observed in phagosomal proteolysis or the ability of the phagosome to acidify in the absence of selenocysteine-containing proteins (Fig. 3F–I). Together, these findings indicate that efficient disulfide reduction in the phagosome is not only dependent on NADPH but also on selenocysteine-containing proteins, such as TR.

Extracellular thiol concentration influences phagosomal disulfide reduction

The effect of depleting NADPH or selenoprotein content only partially decreased phagosomal disulfide reduction (25–30%). In addition to intracellular redox factors that may influence phagosomal disulfide reduction, redox factors present in the extracellular environment may influence reductive capacity. In particular, exposure to extracellular concentrations of Cys and/or CySS could influence phagosomal thiol-dependent processes during internalization of the phagocytic target and subsequent maturation of the phagosome. In addition, the influence of the reduction potential is assumed to have a major impact on thiol-dependent activity [2]. Within tissues, the extracellular Cys:CySS couple is estimated to be 8–10 μM:40–50 μM (~1:5 molar ratio) [37]. In comparison, the cytosolic Cys:CySS ratio is ~125 μM:30 μM (~4:1 ratio) [38]. With the use of the Nernst equation at physiologic pH values, these ratios correspond to reduction potentials of approximately −80 and −140 mV, respectively. Therefore, we tested whether the extracellular thiol concentration, the modulation of the extracellular reduction potential, or the type of extracellular thiols present would influence phagosomal disulfide reduction. To accomplish this, $Cybb^{-/-}$ BMMØs were exposed to 0.1×, 1×, and 10× of the approximate physiologic concentrations of Cys:CySS at a molar ratio of 1:5 and 4:1 (corresponding to the approximate molar ratio of extracellular milieu and cytosol, respectively); GSH:GSSG at a molar ratio of 20:1; GSH:GSSG (corresponding to the approximate molar ratio of plasma); and a combination of Cys:CySS and GSH:GSSG couples. Rates of phagosomal disulfide reduction were enhanced with an increasing concentration of extracellular Cys (**Fig. 4A**, black bars). Interestingly, reduction potential had little influence on phagosomal disulfide reduction, as no differences were observed between media containing relatively oxidizing (1:5 Cys:CySS molar ratio) or reducing (4:1 Cys:CySS molar ratio) reduction potentials at similarly increasing concentrations of Cys (Fig. 4A, black vs. gray bars). The exposure of BMMØs to approximate plasma concentrations of GSH:GSSG (2.8 μM:0.14 μM, 20:1 molar ratio, −140 mV) [39] had no significant effect on phagosomal disulfide reduction, alone or in combination with Cys:CySS (Fig. 4A, horizontal and vertical stripe bars, respectively). Consistent with previous studies, no significant differences were observed in proteolysis in $Cybb^{-/-}$ BMMØs at physiologic concentrations of extracellular Cys:CySS (1× Cys:CySS; Fig. 4B, black bars) [40]. However, at superphysiological levels of Cys:CySS concentration (10× Cys:CySS), phagosomal proteolysis was decreased. We also evaluated whether

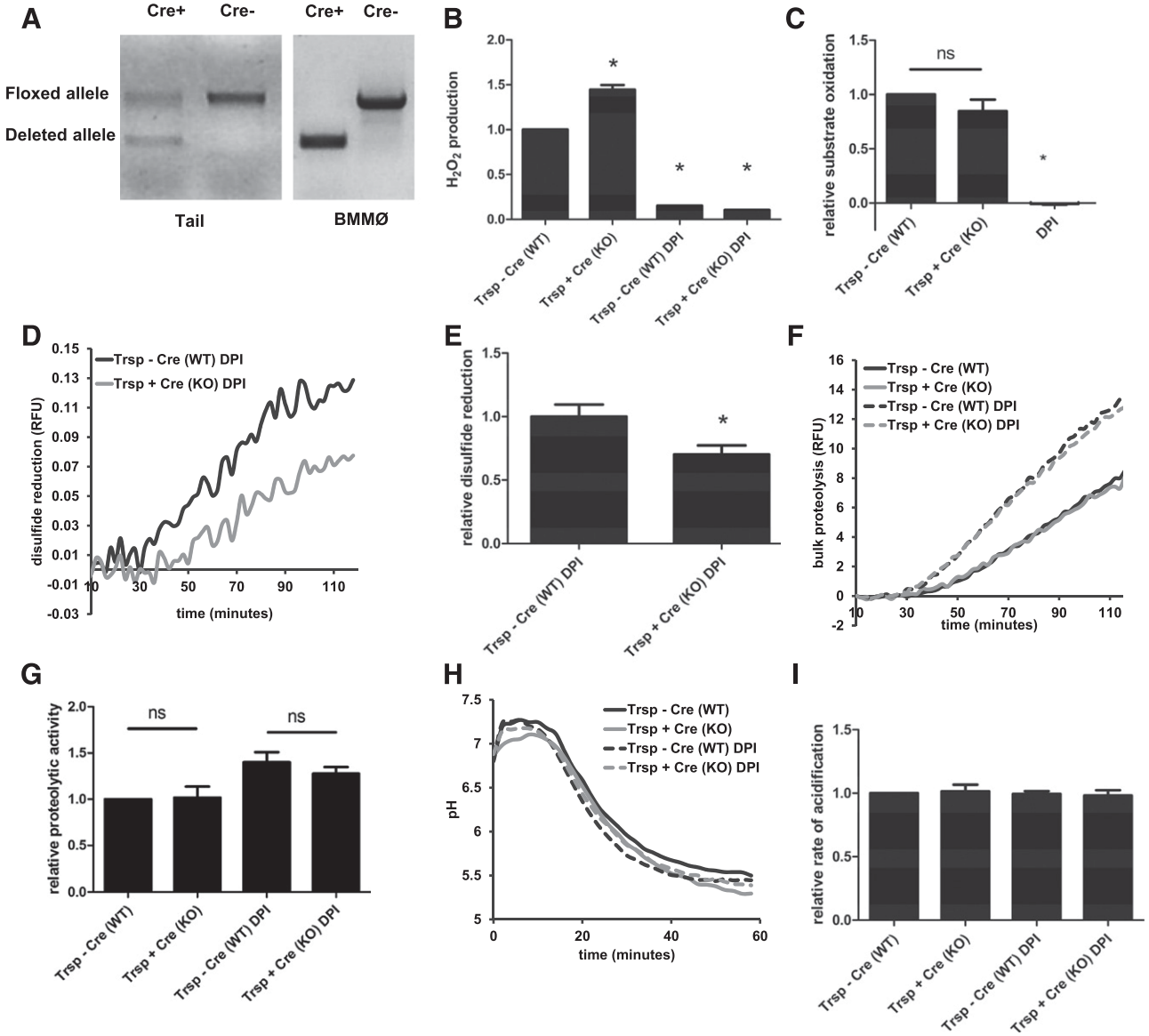

Figure 3. Conditional depletion of selenocysteine-containing proteins decreases phagosomal disulfide reduction. BMMØs, derived from $Trsp^{fl/fl}$/LysM-$Cre^{+/-}$ [*Trsp* knockout (KO)] and $Trsp^{fl/fl}$/LysM-$Cre^{-/-}$ (WT control) mice were used to assess putative involvement of selenoproteins in phagosomal thiol-dependent processes. Ten minutes before addition and subsequent phagocytosis of experimental particles, BMMØs were treated with the NOX2 inhibitor DPI (0.5 μM) where indicated. (A) PCR genotyping of the $Trsp^{fl/fl}$ allele in tail samples and fully differentiated BMMØs. Removal of the floxed site is indicated by a decrease in PCR band size. (B) Extracellular H_2O_2 production relative to $Trsp^{fl/fl}$/LysM-$Cre^{-/-}$ control after phagocytosis of serum-opsonized zymosan particles, as measured by oxidation of the Amplex UltraRed reagent (5 independent experiments. (C) Phagosomal oxidation of the OxyBURST Green H_2HFF BSA substrate conjugated to IgG-opsonized experimental particles (6 independent experiments). (D and E) Phagosomal disulfide reduction of the BODIPY FL L-CySS substrate conjugated to IgG-opsonized experimental particles (9 independent experiments). (F and G) Phagosomal proteolysis of the DQ-albumin substrate conjugated to IgG-opsonized experimental particles (6 independent experiments). (H and I) Phagosomal pH calculated from excitation ratios of the pH-sensitive carboxyfluorescein-SE conjugated to experimental particles by regression to a standard curve (4 independent experiments. (D, F, and H) Representative real-time traces. RFU values are proportional to the degree of substrate reduction/proteolysis. (C, E, G, and I) Averaged rates relative to WT controls are shown for each phagosomal measurement. Relative rates of phagosomal ROS production were calculated between 30 and 80 min after particle internalization. Average relative rates of disulfide reduction and proteolysis were calculated between 60 and 80 min and 40 and 60 min after particle internalization, respectively. Relative rates of phagosomal acidification were calculated between 10 and 15 min after particle internalization. Error bars denote SEM. $^*P < 0.05$.

extracellular thiols could restore disulfide reduction in macrophages conditionally depleted of selenoproteins. Phagosomal disulfide reduction was measured in $Trsp^{fl/fl}$/LysM-$Cre^{+/-}$ BMMØs exposed to increasing concentrations of Cys:CySS (1:5). Supplementation of Cys:CySS to physiologic extracellular concentrations partially restored phagosomal disulfide reduction in selenocysteine-deficient BMMØs (12.9 ± 2.1 and 27.1 ± 4.7% decreases compared with $Trsp^{fl/fl}$/LysM-$Cre^{-/-}$ (WT) controls,

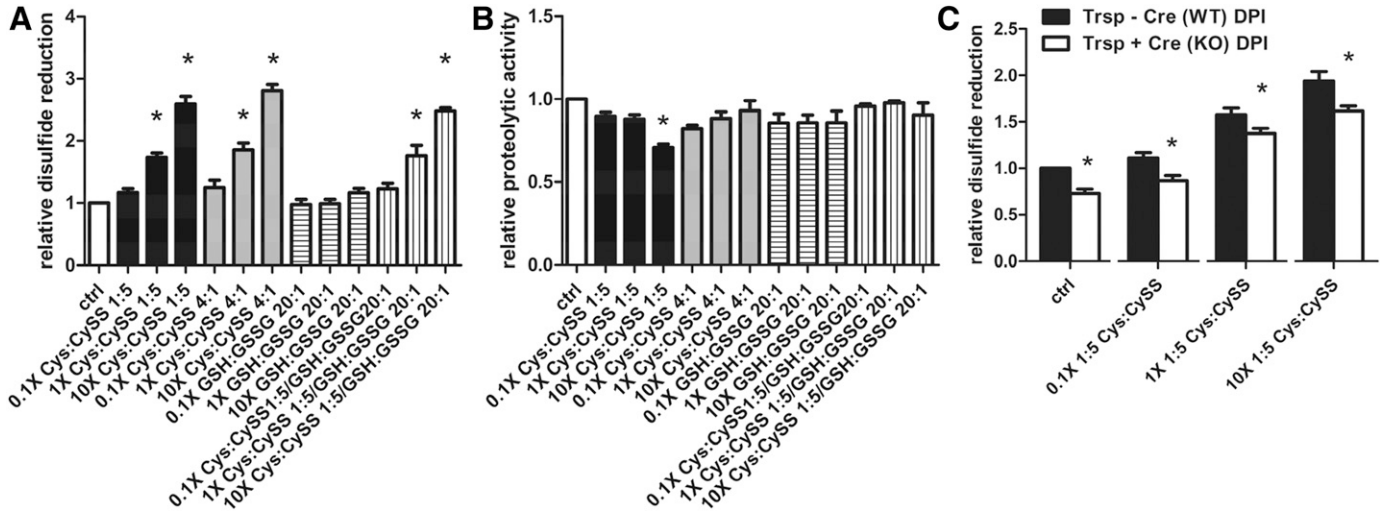

Figure 4. Extracellular Cys concentration influences phagosome-specific disulfide reduction. BMMØs, derived from Cybb$^{-/-}$ mice, were exposed to various concentrations and ratios of extracellular redox couples before and for the duration of phagosome assessment. (A) Phagosomal disulfide reduction of the BODIPY FL L-CySS substrate conjugated to IgG-opsonized experimental particles in Cybb$^{-/-}$ BMMØs. (B) Phagosomal proteolysis of the DQ-albumin substrate conjugated to IgG-opsonized experimental particles in Cybb$^{-/-}$ BMMØs. (C) Phagosomal disulfide reduction by BMMØs derived from Trsp$^{fl/fl}$/LysM-Cre$^{+/-}$ (*Trsp* knockout) and Trsp$^{fl/fl}$/LysM-Cre$^{-/-}$ (control) mice in the presence of various concentrations of Cys:CySS at a molar ratio of 1:5. Average relative rates of disulfide reduction and proteolysis were calculated between 40 and 60 min after particle internalization. Error bars denote SEM of 4 independent experiments. *$P < 0.05$.

respectively; Fig. 4C). These results indicate that the extracellular concentration of Cys, but not physiologic levels of GSH or the redox potential of the extracellular space, significantly contributes to the reductive capacity of the phagosome and supplements contributions by cytosolic selenoprotein-dependent pathways.

DISCUSSION

Despite intense interest in the redox homeostasis of subcellular microenvironments, the systems involved in providing the reductive energy of endosomes, lysosomes, and phagosomes have escaped investigation. It had been postulated previously that the reductive potential of lysosomes may be maintained by Cys/CySS exchange with the cytosol [2, 41, 42]. However, since this system was proposed in 1990, the stoichiometry of Cys as sole reductive source has been questioned, and the lysosomal Cys transporter (on which the proposed mechanism relies) has not been identified [2, 43]. With the use of phagosome-specific probes to monitor thiol-dependent reactions within the lumen of phagolysosomes, we have provided evidence that endogenous and exogenous pathways act to maintain the reductive capacity of these vesicles. Moreover, our findings implicate the NADPH/pentose phosphate pathway as an important endogenous source of reductive energy for the phagolysosome and suggest that the use of NADPH requires at least 1 selenocysteine-containing protein. Our findings also implicate Cys as an important exogenous source of reductive equivalents that can be used by thiol-dependent reactions within the phagosome.

NADPH is a major source of reducing equivalents for most major cellular redox processes, but its involvement with redox homeostasis in the endolysosomal network was not explored previously. Here, we show that the depletion of NADPH impacts disulfide reduction and proteolysis within maturing phagosomes through a pathway that is independent of GSH. Interestingly, NADPH has been shown to support the activity of the Cys protease papain through TR/Trx in a reconstituted system, although evidence for direct interaction of these enzymes and lysosomal Cys cathepsins is lacking and unlikely given our current understanding of lysosomal composition [44]. As NADPH is physically separated from the lumenal microenvironment of phagosomes and lysosomes, how NADPH is used to support thiol-dependent processes within these compartments remains unknown. It is probable that the reductive energy is derived originally through the oxidation of cytosolic NADPH, possibly by the selenocysteine-containing enzyme TR, and is transferred to the phagosomal/lysosomal lumen through intermediate oxidoreductases and lipid-soluble carriers. Consistent with this notion, we demonstrated that knockdown of selenocysteine proteins also decreased rates of phagosomal disulfide reduction at an extent comparable with that of NADPH depletion. Selenocysteine-containing proteins perform a variety of redox-related functions. Although there are 25 selenoproteins in the human proteome and 24 selenoproteins in the murine proteome, only a handful possesses motifs of prototypical oxidoreductases [45]. In BMMØs, well-represented selenoproteins of note are GSH peroxidases 1 and 4 and TR 1 [36]. Whereas our data demonstrate the involvement of the selenoproteome in maintaining the reductive capacity of phagosomes, we fall short of definitively implicating TR in this role. The absence of GSH peroxidases most likely accounts for the observed increase in cytoplasmic steady-state ROS levels in Trsp$^{fl/fl}$/LysM-Cre$^{+/+}$ macrophages [36], as well as the increased H_2O_2 secretion in Trsp$^{fl/fl}$/LysM-Cre$^{+/-}$ macrophages observed in this study. Given that GSH depletion did not impact rates of phagosomal disulfide reduction, a direct link between

peroxidase activity and phagosomal disulfide reduction would be unlikely.

In addition to endogenous sources of reducing equivalents, these data indicate that physiologic levels of exogenous Cys act to support thiol-dependent chemistries within the maturing phagosome. Extracellular Cys may directly reduce disulfides in the early phagosome when the phagosomal lumen is briefly exposed to a neutral pH; however, as a result of the high p*K*a of Cys, its effect on phagosomal disulfide reduction at an acidic pH likely requires an enzyme catalyst, such as GILT [2]. Interestingly, phagosomal disulfide reduction was unaffected by the concentration of CySS present in the extracellular medium. This indicates that thiol:disulfide ratios and subsequent reduction potentials present in the extracellular space have negligible effects on the disulfide reductase activity in the phagosome and that any influence of extracellular thiol:disulfide ratios on phagosomal disulfide reduction are solely dependent on the concentration of Cys. This observation supports a previous study that found that modulation of reduction potentials did not significantly impact thiol-dependent protease activity [46]. In line with previous predictions that Cys is the major reductive currency within lysosomes, extracellular GSH at physiologically relevant concentrations had little effect on phagosomal disulfide reduction.

Levels of phagosomal proteolysis and disulfide reduction have major implications in the processing of protein-based antigens and subsequent presentation to lymphocytes during an adaptive immune response [47]. To date, with respect to redox influence on antigen processing, most attention has been given to the oxidative capacity of the phagosome, particularly the generation of ROS by NOX2 [3]. Oxidative inactivation of thiol-dependent phagosomal proteases, such as cathepsins S and L, has been shown to alter the peptide repertoires available for MHC class II loading and presentation, which in turn, can determine whether $CD4^+$ T cells can to respond to particular epitopes [48]. Other groups have also shown the influence of NOX2-generated ROS on antigen proteolysis in cross-presentation [49, 50]. In addition to proteolysis, the reduction of disulfides within antigens has been shown to be a key step in their processing [1]. Although hitherto little work has been dedicated to determine the pathways that provide the reductive energy to endolysosomal system, the role of GILT for catalyzing disulfide reduction within these compartments is well established. GILT has been shown to be necessary for the processing of various disulfide-containing model antigens and to influence the composition of antigenic peptide repertoires [51–53]. In addition to the reduction of disulfides within antigens, GILT may influence antigen processing by modulating the relative activities of lysosomal proteases. Indeed, it has been shown that GILT supports the activity of cathepsin S in alternatively activated BMMØs, which may contribute to the elevated levels of phagosomal proteolysis in these cells [7]. The underpinning of both of these key steps in antigen processing—thiol-dependent proteolysis and disulfide reduction—is the availability of reducing equivalents within endosomes, lysosomes, and phagosomes. It is reasonable to assume that modulation of the sources and pathways that provide these reducing equivalents would have profound effects on antigen processing, in addition to the basic functioning of these organelles.

Overall, there is likely to be a variety of networks that contribute to endosomal/lysosomal/phagosomal reductive capacity, including thiol:disulfide couples, redox enzymes, and other electron transport/transfer systems. This study indicates that endogenous and exogenous sources supply reductive energy to the phagosome and will hopefully serve to guide future characterization of pathways that act to maintain the redox homeostasis of endosomes, lysosomes, and phagosomes.

AUTHORSHIP

D.R.B. and R.M.Y. conceived of and designed the experiments, analyzed results, and wrote the paper. D.R.B., C.J.G., and P.T. performed experiments.

ACKNOWLEDGMENTS

This work was supported by the Canadian Institutes of Health Research and Natural Sciences and Engineering Research Council of Canada. The authors thank Dr. Dolph Hatfield (U.S. National Institutes of Health) for the provision of the *Trsp*$^{fl/fl}$ mice.

DISCLOSURES

The authors declare no conflicts of interest.

REFERENCES

1. Collins, D. S., Unanue, E. R., Harding, C. V. (1991) Reduction of disulfide bonds within lysosomes is a key step in antigen processing. *J. Immunol.* **147,** 4054–4059.
2. Pillay, C. S., Elliott, E., Dennison, C. (2002) Endolysosomal proteolysis and its regulation. *Biochem. J.* **363,** 417–429.
3. Yates, R. M. (2013) Redox considerations in the phagosome: current concepts, controversies, and future challenges. *Antioxid. Redox Signal.* **18,** 628–629.
4. Kotsias, F., Hoffmann, E., Amigorena, S., Savina, A. (2013) Reactive oxygen species production in the phagosome: impact on antigen presentation in dendritic cells. *Antioxid. Redox Signal.* **18,** 714–729.
5. Lockwood, T. D. (2002) Cathepsin B responsiveness to glutathione and lipoic acid redox. *Antioxid. Redox Signal.* **4,** 681–691.
6. Maric, M., Arunachalam, B., Phan, U. T., Dong, C., Garrett, W. S., Cannon, K. S., Alfonso, C., Karlsson, L., Flavell, R. A., Cresswell, P. (2001) Defective antigen processing in GILT-free mice. *Science* **294,** 1361–1365.
7. Balce, D. R., Allan, E. R., McKenna, N., Yates, R. M. (2014) γ-Interferon-inducible lysosomal thiol reductase (GILT) maintains phagosomal proteolysis in alternatively activated macrophages. *J. Biol. Chem.* **289,** 31891–31904.
8. Phan, U. T., Arunachalam, B., Cresswell, P. (2000) Gamma-interferon-inducible lysosomal thiol reductase (GILT). Maturation, activity, and mechanism of action. *J. Biol. Chem.* **275,** 25907–25914.
9. Jensen, P. E. (1991) Reduction of disulfide bonds during antigen processing: evidence from a thiol-dependent insulin determinant. *J. Exp. Med.* **174,** 1121–1130.
10. Singh, R., Cresswell, P. (2010) Defective cross-presentation of viral antigens in GILT-free mice. *Science* **328,** 1394–1398.
11. Go, Y. M., Jones, D. P. (2008) Redox compartmentalization in eukaryotic cells. *Biochim. Biophys. Acta* **1780,** 1273–1290.
12. Lockwood, T. D. (2000) Redox control of protein degradation. *Antioxid. Redox Signal.* **2,** 851–878.
13. Lockwood, T. D. (2013) Lysosomal metal, redox and proton cycles influencing the CysHis cathepsin reaction. *Metallomics* **5,** 110–124.
14. Kumaraswamy, E., Carlson, B. A., Morgan, F., Miyoshi, K., Robinson, G. W., Su, D., Wang, S., Southon, E., Tessarollo, L., Lee, B. J., Gladyshev, V. N., Hennighausen, L., Hatfield, D. L. (2003) Selective removal of the selenocysteine tRNA [Ser]Sec gene (Trsp) in mouse mammary epithelium. *Mol. Cell. Biol.* **23,** 1477–1488.
15. Yates, R. M., Russell, D. G. (2008) Real-time spectrofluorometric assays for the lumenal environment of the maturing phagosome. *Methods Mol. Biol.* **445,** 311–325.

16. VanderVen, B. C., Yates, R. M., Russell, D. G. (2009) Intraphagosomal measurement of the magnitude and duration of the oxidative burst. *Traffic* **10,** 372–378.
17. Rybicka, J. M., Balce, D. R., Khan, M. F., Krohn, R. M., Yates, R. M. (2010) NADPH oxidase activity controls phagosomal proteolysis in macrophages through modulation of the lumenal redox environment of phagosomes. *Proc. Natl. Acad. Sci. USA* **107,** 10496–10501.
18. Baird, S. K., Reid, L., Hampton, M. B., Gieseg, S. P. (2005) OxLDL induced cell death is inhibited by the macrophage synthesised pterin, 7,8-dihydroneopterin, in U937 cells but not THP-1 cells. *Biochim. Biophys. Acta* **1745,** 361–369.
19. Hu, M. L. (1994) Measurement of protein thiol groups and glutathione in plasma. *Methods Enzymol.* **233,** 380–385.
20. Balce, D. R., Yates, R. M. (2013) Redox-sensitive probes for the measurement of redox chemistries within phagosomes of macrophages and dendritic cells. *Redox Biol.* **1,** 467–474.
21. Fang, J., Lu, J., Holmgren, A. (2005) Thioredoxin reductase is irreversibly modified by curcumin: a novel molecular mechanism for its anticancer activity. *J. Biol. Chem.* **280,** 25284–25290.
22. O'Donnell, B. V., Tew, D. G., Jones, O. T., England, P. J. (1993) Studies on the inhibitory mechanism of iodonium compounds with special reference to neutrophil NADPH oxidase. *Biochem. J.* **290,** 41–49.
23. Zhao, R., Holmgren, A. (2004) Ebselen is a dehydroascorbate reductase mimic, facilitating the recycling of ascorbate via mammalian thioredoxin systems. *Antioxid. Redox Signal.* **6,** 99–104.
24. Fang, J., Zhong, L., Zhao, R., Holmgren, A. (2005) Ebselen: a thioredoxin reductase-dependent catalyst for alpha-tocopherol quinone reduction. *Toxicol. Appl. Pharmacol.* **207** (2: Suppl) 103–109.
25. Zhao, R., Masayasu, H., Holmgren, A. (2002) Ebselen: a substrate for human thioredoxin reductase strongly stimulating its hydroperoxide reductase activity and a superfast thioredoxin oxidant. *Proc. Natl. Acad. Sci. USA* **99,** 8579–8584.
26. Arnér, E. S. (2009) Focus on mammalian thioredoxin reductases—important selenoproteins with versatile functions. *Biochim. Biophys. Acta* **1790,** 495–526.
27. Smith, A. D., Guidry, C. A., Morris, V. C., Levander, O. A. (1999) Aurothioglucose inhibits murine thioredoxin reductase activity in vivo. *J. Nutr.* **129,** 194–198.
28. Omata, Y., Folan, M., Shaw, M., Messer, R. L., Lockwood, P. E., Hobbs, D., Bouillaguet, S., Sano, H., Lewis, J. B., Wataha, J. C. (2006) Sublethal concentrations of diverse gold compounds inhibit mammalian cytosolic thioredoxin reductase (TrxR1). *Toxicol. In Vitro* **20,** 882–890.
29. Balce, D. R., Li, B., Allan, E. R., Rybicka, J. M., Krohn, R. M., Yates, R. M. (2011) Alternative activation of macrophages by IL-4 enhances the proteolytic capacity of their phagosomes through synergistic mechanisms. *Blood* **118,** 4199–4208.
30. Gunatilleke, S. S., Barrios, A. M. (2006) Inhibition of lysosomal cysteine proteases by a series of Au(I) complexes: a detailed mechanistic investigation. *J. Med. Chem.* **49,** 3933–3937.
31. Arnér, E. S., Björnstedt, M., Holmgren, A. (1995) 1-Chloro-2,4-dinitrobenzene is an irreversible inhibitor of human thioredoxin reductase. Loss of thioredoxin disulfide reductase activity is accompanied by a large increase in NADPH oxidase activity. *J. Biol. Chem.* **270,** 3479–3482.
32. Seyfried, J., Wüllner, U. (2007) Inhibition of thioredoxin reductase induces apoptosis in neuronal cell lines: role of glutathione and the MKK4/JNK pathway. *Biochem. Biophys. Res. Commun.* **359,** 759–764.
33. Hothersall, J. S., Gordge, M., Noronha-Dutra, A. A. (1998) Inhibition of NADPH supply by 6-aminonicotinamide: effect on glutathione, nitric oxide and superoxide in J774 cells. *FEBS Lett.* **434,** 97–100.
34. Deneke, S. M., Fanburg, B. L. (1989) Regulation of cellular glutathione. *Am. J. Physiol.* **257,** L163–L173.
35. Carlson, B. A., Yoo, M. H., Tsuji, P. A., Gladyshev, V. N., Hatfield, D. L. (2009) Mouse models targeting selenocysteine tRNA expression for elucidating the role of selenoproteins in health and development. *Molecules* **14,** 3509–3527.
36. Carlson, B. A., Yoo, M. H., Sano, Y., Sengupta, A., Kim, J. Y., Irons, R., Gladyshev, V. N., Hatfield, D. L., Park, J. M. (2009) Selenoproteins regulate macrophage invasiveness and extracellular matrix-related gene expression. *BMC Immunol.* **10,** 57.
37. Jones, D. P., Mody, V. C., Jr., Carlson, J. L., Lynn, M. J., Sternberg, P., Jr. (2002) Redox analysis of human plasma allows separation of pro-oxidant events of aging from decline in antioxidant defenses. *Free Radic. Biol. Med.* **33,** 1290–1300.
38. Jones, D. P., Go, Y. M., Anderson, C. L., Ziegler, T. R., Kinkade, Jr., J. M., Kirlin, W. G. (2004) Cysteine/cystine couple is a newly recognized node in the circuitry for biologic redox signaling and control. *FASEB J.* **18,** 1246–1248.
39. Jones, D. P., Carlson, J. L., Mody, V. C., Cai, J., Lynn, M. J., Sternberg, P. (2000) Redox state of glutathione in human plasma. *Free Radic. Biol. Med.* **28,** 625–635.
40. Rybicka, J. M., Balce, D. R., Chaudhuri, S., Allan, E. R., Yates, R. M. (2012) Phagosomal proteolysis in dendritic cells is modulated by NADPH oxidase in a pH-independent manner. *EMBO J.* **31,** 932–944.
41. Pisoni, R. L., Thoene, J. G. (1991) The transport systems of mammalian lysosomes. *Biochim. Biophys. Acta* **1071,** 351–373.
42. Pisoni, R. L., Acker, T. L., Lisowski, K. M., Lemons, R. M., Thoene, J. G. (1990) A cysteine-specific lysosomal transport system provides a major route for the delivery of thiol to human fibroblast lysosomes: possible role in supporting lysosomal proteolysis. *J. Cell Biol.* **110,** 327–335.
43. Lloyd, J. B. (1992) Lysosomal handling of cystine residues: stoichiometry of cysteine involvement. *Biochem. J.* **286,** 979–980.
44. Stephen, A. G., Powls, R., Beynon, R. J. (1993) Activation of oxidized cysteine proteinases by thioredoxin-mediated reduction in vitro. *Biochem. J.* **291,** 345–347.
45. Kryukov, G. V., Castellano, S., Novoselov, S. V., Lobanov, A. V., Zehtab, O., Guigó, R., Gladyshev, V. N. (2003) Characterization of mammalian selenoproteomes. *Science* **300,** 1439–1443.
46. Jordans, S., Jenko-Kokalj, S., Kühl, N. M., Tedelind, S., Sendt, W., Brömme, D., Turk, D., Brix, K. (2009) Monitoring compartment-specific substrate cleavage by cathepsins B, K, L, and S at physiological pH and redox conditions. *BMC Biochem.* **10,** 23.
47. Blum, J. S., Wearsch, P. A., Cresswell, P. (2013) Pathways of antigen processing. *Annu. Rev. Immunol.* **31,** 443–473.
48. Allan, E. R., Tailor, P., Balce, D. R., Pirzadeh, P., McKenna, N. T., Renaux, B., Warren, A. L., Jirik, F. R., Yates, R. M. (2014) NADPH oxidase modifies patterns of MHC class II-restricted epitopic repertoires through redox control of antigen processing. *J. Immunol.* **192,** 4989–5001.
49. Savina, A., Jancic, C., Hugues, S., Guermonprez, P., Vargas, P., Moura, I. C., Lennon-Duménil, A. M., Seabra, M. C., Raposo, G., Amigorena, S. (2006) NOX2 controls phagosomal pH to regulate antigen processing during crosspresentation by dendritic cells. *Cell* **126,** 205–218.
50. Crotzer, V. L., Matute, J. D., Arias, A. A., Zhao, H., Quilliam, L. A., Dinauer, M. C., Blum, J. S. (2012) Cutting edge: NADPH oxidase modulates MHC class II antigen presentation by B cells. *J. Immunol.* **189,** 3800–3804.
51. West, L. C., Cresswell, P. (2013) Expanding roles for GILT in immunity. *Curr. Opin. Immunol.* **25,** 103–108.
52. Haque, M. A., Li, P., Jackson, S. K., Zarour, H. M., Hawes, J. W., Phan, U. T., Maric, M., Cresswell, P., Blum, J. S. (2002) Absence of gamma-interferon-inducible lysosomal thiol reductase in melanomas disrupts T cell recognition of select immunodominant epitopes. *J. Exp. Med.* **195,** 1267–1277.
53. Bogunovic, B., Srinivasan, P., Ueda, Y., Tomita, Y., Maric, M. (2010) Comparative quantitative mass spectrometry analysis of MHC class II-associated peptides reveals a role of GILT in formation of self-peptide repertoire. *PLoS One* **5,** e10599.

KEY WORDS:
redox · reductase · proteolysis · endosome · lysosome